JOURNAL OF MATERIALS SCIENCE 28 (1993) 5301–5312

Mechanism and kinetics of the chemical interaction between liquid aluminium and silicon-carbide single crystals

J. C. VIALA, F. BOSSELET
Laboratoire de Physico-chimie Minérale 1, URA CNRS 116, Université Claude Bernard Lyon 1, 69622 Villeurbanne Cedex, France

V. LAURENT
Laboratoire de Thermodynamique et Physico-chimie Métallurgiques, URA CNRS 29, ENSEEG, 38402 Saint Martin D'Hères Cedex, France

Y. LEPETITCORPS
Laboratoire de Chimie du solide du CNRS, Université Bordeaux 1, 33405 Talence Cedex, France

Previous investigations of phase equilibria in the ternary system Al–C–Si have shown that silicon carbide is attacked by pure aluminium at temperatures higher or equal to 923 ± 3 K and up to about 1600 K, according to the chemical reaction:

$$4Al + 3SiC \leftrightarrow Al_4C_3 + 3Si$$

In the present work, a study has been carried out to obtain more detailed information on the mechanism and kinetics of this reaction. For that purpose, 6H silicon carbide platelets with broad Si (0 0 0 1) and C (0 0 0 $\bar{1}$) faces were isothermally heated at 1000 K in a large excess of liquid aluminium. Characterization of the resulting samples by Auger electron spectroscopy (AES) and scanning electron microscopy (SEM) revealed that the reaction proceeds in both faces via a dissolution–precipitation mechanism. However, the polarity of the substrate surface strikingly influences the rate at which silicon carbide decomposes: dissolution starts much more rapidly on the Si face than on the C face, but, while a barrier layer of aluminium carbide is formed on the Si face protecting it against further attack, the major part of the C face remains directly exposed to liquid aluminium and thus may continue to dissolve at a low but constant rate up to complete decomposition of the α-SiC crystal.

1. Introduction

The recent development of composite materials made of an aluminium-base matrix reinforced with silicon carbide particles, whiskers or fibres has given grounds for substantial research on the physical and chemical phenomena occurring at the metal/carbide interface during hot-processing or use of these materials. Among these phenomena, chemical reactivity, which largely influences the mechanical properties of this type of composites, has been the subject of numerous investigations [1–14].

These studies have led to the conclusion that the Al/SiC interface exhibits a good chemical stability at temperatures lower than about 870 K [4, 7, 8] whereas it becomes reactive at temperatures where aluminium is in the liquid state, i.e. at temperatures higher than 933 K [1, 2, 5, 6, 8–14]. In the latter case, aluminium carbide, Al_4C_3, and silicon were characterized as reaction products up to about 1600 K. However, neither the thermodynamic principles governing the chemical interaction between aluminium and SiC nor the mechanism and kinetics of the reaction process were thoroughly investigated.

As far as the thermodynamics is concerned, significant progress has recently been made towards a better understanding of this interaction. High-temperature isothermal sections ($T > 2200$ K) of the Al–C–Si ternary-phase diagram have been experimentally determined by Oden and McCune [15] and recalculated by Lukas [16]. Moreover, a model based on stable and metastable phase equilibria has been developed in our laboratory [17] for describing the Al–SiC interaction at the medium and low temperatures which are of interest in composite manufacture. According to this model, SiC is in thermodynamic equilibrium with solid aluminium (Fig. 1a) at every temperature lower than 923 K (pressure, $p = 1$ atm). At 923 ± 3 K, the following invariant transformation occurs in the Al–C–Si system (Fig. 1c):

$$SiC + Al \leftrightarrow Al_4C_3 + L_0$$

L_0 is a ternary liquid phase containing aluminium (the

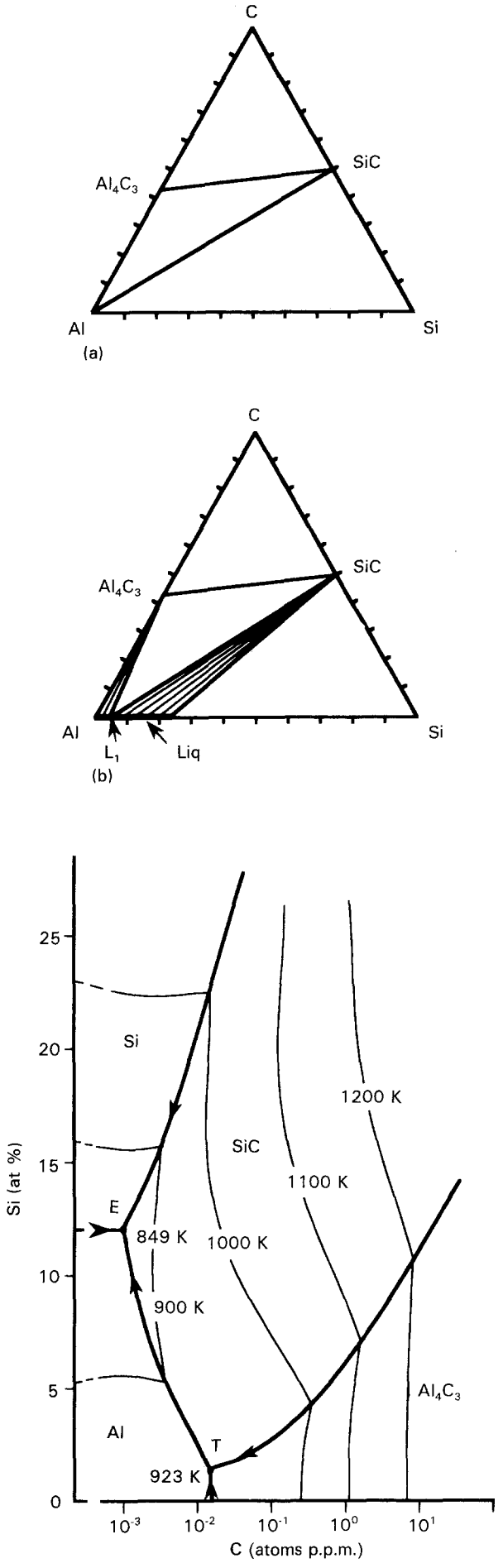

Figure 1. Metastable Al–C–Si phase diagram describing the chemical interaction between Al and SiC at low temperatures ($T < 1620$ K): (a) isothermal section at 840 K, (b) isothermal section at 1000 K, and (c) liquidus projection of the Al-rich corner.

major constituent), silicon (1.5 ± 0.4 at %) and carbon (less than 1 atomic p.p.m. – part per million). At temperatures higher than 923 K and up to about 1600 K, solid ($923 < T < 933$ K) or liquid aluminium ($T > 933$ K) reacts with SiC, producing Al_4C_3 and silicon. If SiC is in excess, a three-phased monovariant equilibrium involving unreacted SiC, Al_4C_3 and a ternary liquid phase, L_1, can be attained (Fig. 1b). The carbon content of this liquid phase, L_1 is simultaneously in equilibrium with SiC and Al_4C_3 and remains very low (about 30 atomic p.p.m. at 1300 K) whereas its silicon content increases with the temperature from 1.5 at % at 923 K to 12.7 at % at 1273 K, as shown by Fig. 1c. Now, if aluminium is in excess, SiC can be entirely decomposed and a two-phased equilibrium between Al_4C_3 and a silicon-poor ternary liquid can be attained (Fig. 1b).

Having established these thermodynamic principles, it became possible to obtain more detailed information on the mechanism and kinetics of the chemical decomposition of SiC by aluminium. It is with this end in view that we have characterized the morphology and composition of the interfacial zone formed by reacting single-crystalline SiC substrates at 930–1100 K in a large excess of aluminium, i.e. in out-of-equilibrium conditions approaching those realized during the liquid infiltration of Al/SiC composites.

2. Experimental procedure

2.1. SiC substrates

The silicon carbide single crystals used in this study were extracted from growth clusters supplied by Elektroschmelzwerk Kempten GmbH. These clusters were prepared by arc-melting of an Al–SiO_2–C mixture (Acheson-furnace process). The substrates appeared as black platelets (mean diameter, 5 mm; thickness, about 1.5 mm) with large hexagonal faces. Auger electron spectroscopy (AES) and secondary-ion mass (SIMS) analyses of some of these platelets revealed that the C/Si atomic ratio was 1.0 ± 0.1 and that apart from an oxygen surface contamination due to natural oxidation (SiO_2) they contained traces of Al (responsible for the black colouring), Cu and S.

X-ray powder diffraction spectra recorded on crushed crystals showed that they were of the α-hexagonal variety and that the 6H polytyp was largely predominant. Further structural characterization by transmission electron microscopy (TEM) revealed that small amounts of the 15R polytyp were also present with some inclusions of aluminium carbide, Al_4C_3.

Fig. 2 shows the arrangement of silicon and carbon atoms in α-hexagonal SiC [18]. It can be seen that SiC crystals have a layered structure consisting of an alternate stacking of planes that are entirely composed of C atoms and planes that are entirely composed of Si atoms. The distance from a C plane to the underlying Si plane is either 0.063 or 0.189 nm, according to the observation direction (parallel to the *c*-axis). This asymmetry results in polar crystals whose (0 0 0 1) and (0 0 0 $\bar{1}$) surfaces are not equivalent. Conventionally, the surface with the indices (0 0 0 1) is called the Si face

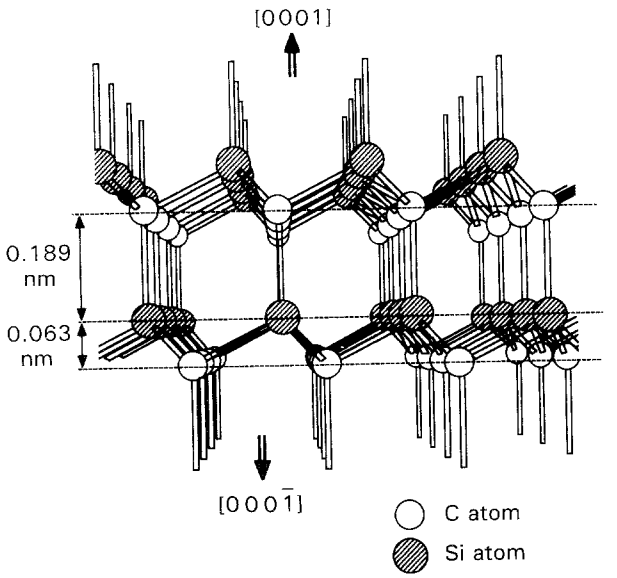

Figure 2. Arrangement of Si and C atoms in α-hexagonal SiC crystals [18].

and that with the indices (000$\bar{1}$) the C face. Large differences in oxidation kinetics have been reported for these two faces: at temperatures ranging from 1170 to 1670 K , the C face oxidizes three to seven times faster than the Si face in dry oxygen or air [19–20]. Relying on these data, preliminary oxidation tests were performed to distinguish the faces of our crystals. SiC platelets were first etched in a dilute HF solution to remove any oxide present and then heated in air at 1273 K for 27 h. Under such conditions, the thickness of the SiO_2 layer grown on the C face was about 100–150 nm, which resulted in a characteristic blue colouring when it was observed in reflected light, whereas the Si face (with an oxide layer thickness of about 15–20 nm) remained black.

After having recognized the C and Si faces, the SiC platelets were cut to an appropriate size using a diamond saw, etched again in a dilute HF solution to remove the SiO_2 oxide layer, rinsed in deionized water and dried. Some experiments were realized using the as-obtained substrates. For other experiments, the Si and C faces received a subsequent polishing whereby a SiC surface layer of about 100 μm was removed. This was achieved by using diamond pastes with particle sizes decreasing from 15 to 0.3μm. After rinsing and drying, the roughness of the resulting surfaces was less than 0.3 μm.

2.2. Sample preparation and characterization

In the first series of experiments, small cubes (of edge 1 mm) of aluminium (purity > 99.99%) were put on either the Si or the C face of polished SiC substrates held horizontally (Fig. 3a). The cube–substrate assemblies were then heated under a high vacuum ($p \approx 5.10^{-5}$ Pa) at 1073 K for 80 min, at 1123 K for 100 min, and at 1148 K for 60 min, successively. Such a procedure allowed contact-angle measurements to be made [21–22]. After cooling to room temperature, an aluminium drop with an average diameter of about 1 mm was solidified onto the Si or C face of the substrates. In order to determine the composition of the metal/carbide interfacial zone by AES, sections at an acute angle to the substrate surface were cut in these samples (Fig. 3b). AES depth profiles were then recorded on these sections for the four elements Al, C, O, Si, with aluminium being etched by argon-ion bombardment at a rate of about 25 nm min^{-1}.

Another series of experiments was carried out with the aim of examining the morphological changes occurring at the metal/carbide interface and at the SiC-substrate surfaces when reaction parameters, such as heating time and temperature, surface preparation or crystal polarity, were modified. For that purpose, SiC substrates were cold pressed under 450 MPa with aluminium powder (purity > 99%, grain size < 100–200 μm, Fluka) in such a way that they were entirely embedded in a parallelepipedic rod (6 × 6 × 30 mm), as shown by Fig. 4. The weight ratio SiC:Al in the resulting rods was about 0.3.

The parallelepipedic rods were then placed in alumina boats and heated in quartz tubes closed under purified argon at 1 atm. The heating assembly was a conventional horizontal-tube furnace equipped with a stability controller. Most of the experiments were made at 1000 K, but some were carried out at 930 and 1100 K. The temperatures were determined with an accuracy better than ± 3 K. At the end of the isothermal treatment, the duration of which varied from 15 min to 1500 h, the quartz tubes containing the samples were rapidly cooled to room temperature in air.

These Al–SiC samples were cut perpendicularly to the Si and C faces of the SiC substrates using a diamond saw and mounted in a plastic resin. The transverse sections thus obtained were polished to a 1 μm diamond finish, rinsed by ultrasonic vibration in anhydrous ethanol and dried. Then, they were kept in ambient air for 12 to 24 h to allow a thin oxidation layer to grow on aluminium carbide, which facilitated further examination of this phase by SEM, using a JEOL 35CF apparatus operated at an accelerating

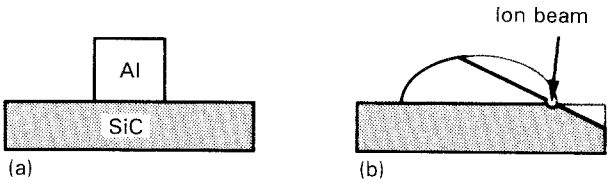

Figure 3. Al-cube/SiC-substrate assembly: (a) before heat treatment, and (b) heat treated and cut for AES characterization.

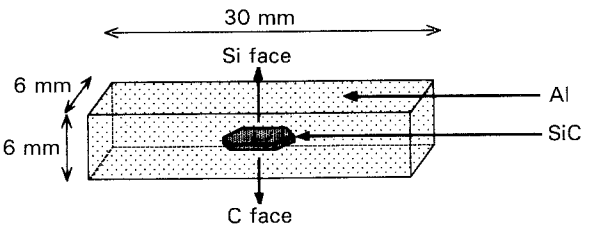

Figure 4. Al–SiC samples prepared for heat treatment and SEM observations.

voltage of 15 kV. Observations were also made of the Si and C surfaces of the SiC substrates, after having extracted the rods from their resin embedding and dissolved aluminium and aluminium carbide by immersion in a 3M HCl solution for 15 h at room temperature.

3. Results and discussion

3.1. AES characterization of the Al/SiC interface

The AES depth profile recorded through the Al/SiC interface formed between the C face of a SiC single crystal and an aluminium drop successively melted at 1073, 1123 and 1148 K on this face is shown in Fig. 5. The left-hand side of the figure corresponds to the aluminium drop, the right-hand side to the SiC substrate. The crossing of the Al/SiC interface occurs for sputtering times ranging from about 30 to 55 min. Since the etching rate of aluminium is about 25 nm min^{-1}, the transition zone would extend over a depth of about 625 nm. As depth profiling has been realized on a skew section, it is, however, uncertain whether this transition zone corresponds to a reaction layer or to a straight interface.

Fig. 6 shows the depth profile of the metal/carbide interface formed at the Si face of a SiC substrate on which an aluminium drop has been melted under the same conditions as previously. The transition zone that can be observed in this case appears much broader: about 5000 nm at the Si face instead of 625 nm at the C face. This proves that a reaction with aluminium has really occurred at the Si face during the heat treatment. The presence of large amounts of aluminium and carbon in the reaction zone is consistent with the formation of aluminium carbide, Al_4C_3. A partial oxidation or hydrolysis of this compound during preparation of the skew section would explain the high oxygen content observed at the beginning of ion-beam etching.

As the aluminium drop was melted for the same time and at the same temperature on each face of the substrate, it is clear at this point that the Si and C faces

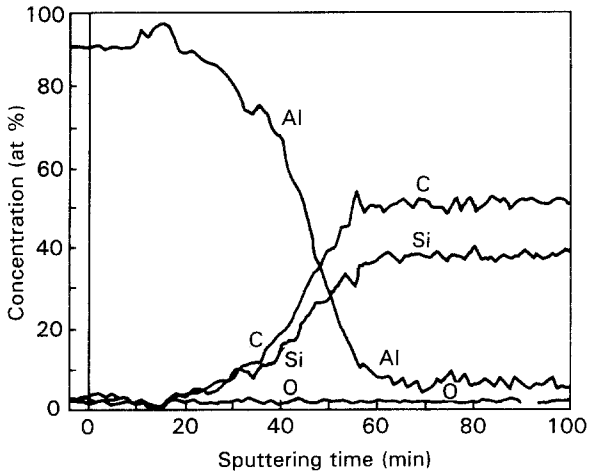

Figure 5. AES depth profile through the Al/SiC interface for an α-hexagonal SiC crystal on whose C face an aluminium drop has been melted. (Sputtering rate = 25 nm min^{-1}.)

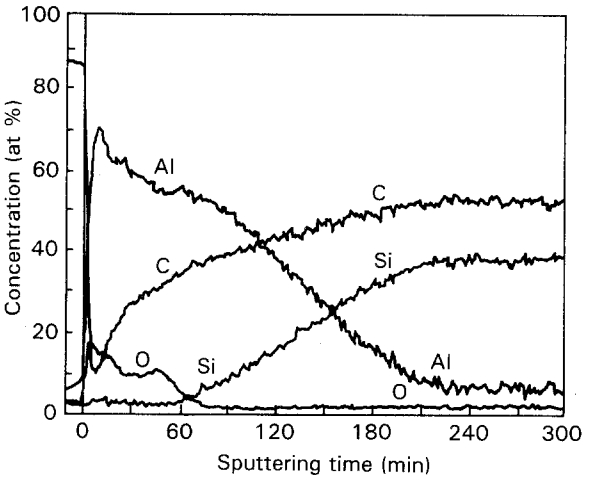

Figure 6. AES depth profile through the Al/SiC interface for an α-hexagonal SiC crystal on whose Si face an aluminium drop has been melted (for the same melting conditions as those realised on the C face). (Sputtering rate = 25 nm min^{-1}.)

of α-SiC crystals exhibit very different chemical reactivities in the presence of liquid aluminium.

3.2. SEM examination of the Al/SiC interface and of the SiC surface

3.2.1. Polished Si surfaces reacted at 1000 K

Systematic observations were made by SEM at the Si face of Al–SiC samples (parallelepipedic rods) heated at 1000 K for times varying from 15 min to 1500 h. In these experiments, the Si face of the α-SiC substrates was mechanically polished prior to cold pressing with Al powder. Transverse sections of the Al/SiC interface at different reaction times are shown in Fig. 7a to e. The corresponding Si surfaces of the α-SiC crystals extracted by chemical dissolution of Al and Al_4C_3 are presented in Fig. 7f to j.

Observation of a transverse section of a sample heated for 15 min at 1000 K shows a nearly flat Al/SiC interface (Fig. 7a). Small Al_4C_3 crystallites with a particle size about 1–2 μm can, however, be distinguished at some points of this interface. These crystallites are attached to the SiC surface and form outgrowths in the Al matrix. SEM examination of the Si surface after chemical dissolution of Al and Al_4C_3 revealed isolated SiC islands with geometrical outlines rising above a very plane SiC surface (Fig. 7). The height of these islands is about 0.5 μm and their lateral extension varies from 1 to 4 μm.

For a reaction time of 1.5 h, the Al_4C_3 crystals which form on the Si face are much bigger than previously. Tabular crystals having an average diameter of about 10 μm and a height of order 2 μm are often encountered, with their basal plane nearly parallel to the SiC substrate surface. Between these crystals, the Si face remained in close contact with aluminium. In these places, SiC was eroded, which results in an apparent substrate-surface roughness of about 2 μm. After chemical dissolution of Al and Al_4C_3 (Fig. 7), the Si face exhibits the same typical morphology as previously, i.e. SiC islands emerging from a flat surface, but the islands are higher (about 2 μm instead of

0.5 μm) and have a larger lateral extension (of order 10 μm, instead of 1–4 μm).

These interface and surface morphologies observed at the Si face of α-SiC crystals heated at 1000 K in an excess of liquid aluminium for short reaction times (15 min and 1.5 h) are characteristic of reactions that proceed via a dissolution–precipitation mechanism. The thermodynamic principles governing such a mechanism can be understood by considering the Al-rich part of the 1000 K Al–C–Si isothermal section in Fig. 8a. When SiC crystals are heated in pure liquid aluminium, they begin to dissolve without formation of any other phase, whereas the molten metal becomes richer in carbon and silicon. As the maximum solubility of carbon in liquid aluminium is very low, about 0.15 atoms p.p.m. at 1000 K according to Simensen [24], this simple dissolution stage is very short, even non-existent. It ends when the concentration of carbon in the liquid phase becomes equal to that of point A: the point lying at the intersection of the Al–SiC line with the L–Al_4C_3 equilibrium curve (Fig. 8a). Then, SiC continues to dissolve while the composition of the liquid phase tends to reach that of point B, the intersection of the Al–SiC line with the metastable prolongation of the L–SiC equilibrium curve (dotted curve in Fig. 8a). Between point A and point B,

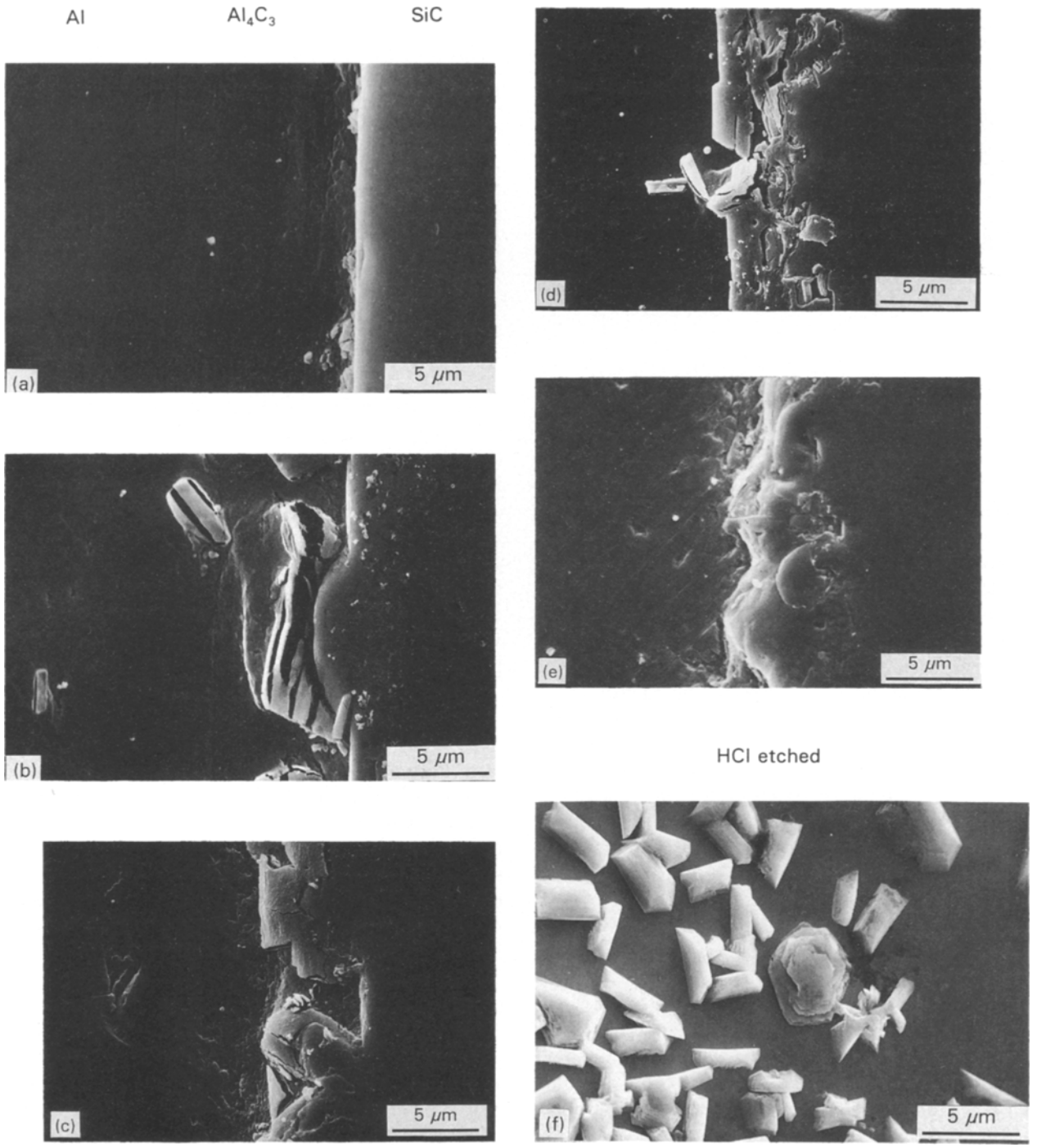

Figure 7. SEM photographs showing the development of the chemical interaction at 1000 K between the Si face of α-hexagonal SiC crystals and liquid aluminium, for reaction times increasing from 15 min to 1500 h, (a)–(e). Transverse sections of the Al/SiC interface and; (f)–(j) Si surface of the SiC crystal after chemical dissolution of Al and Al_4C_3: (a), (f) 15 min; (b), (g) 1.5 h; (c), (h) 15 h; (d), (i) 150 h; and (e), (j) 1500 h.

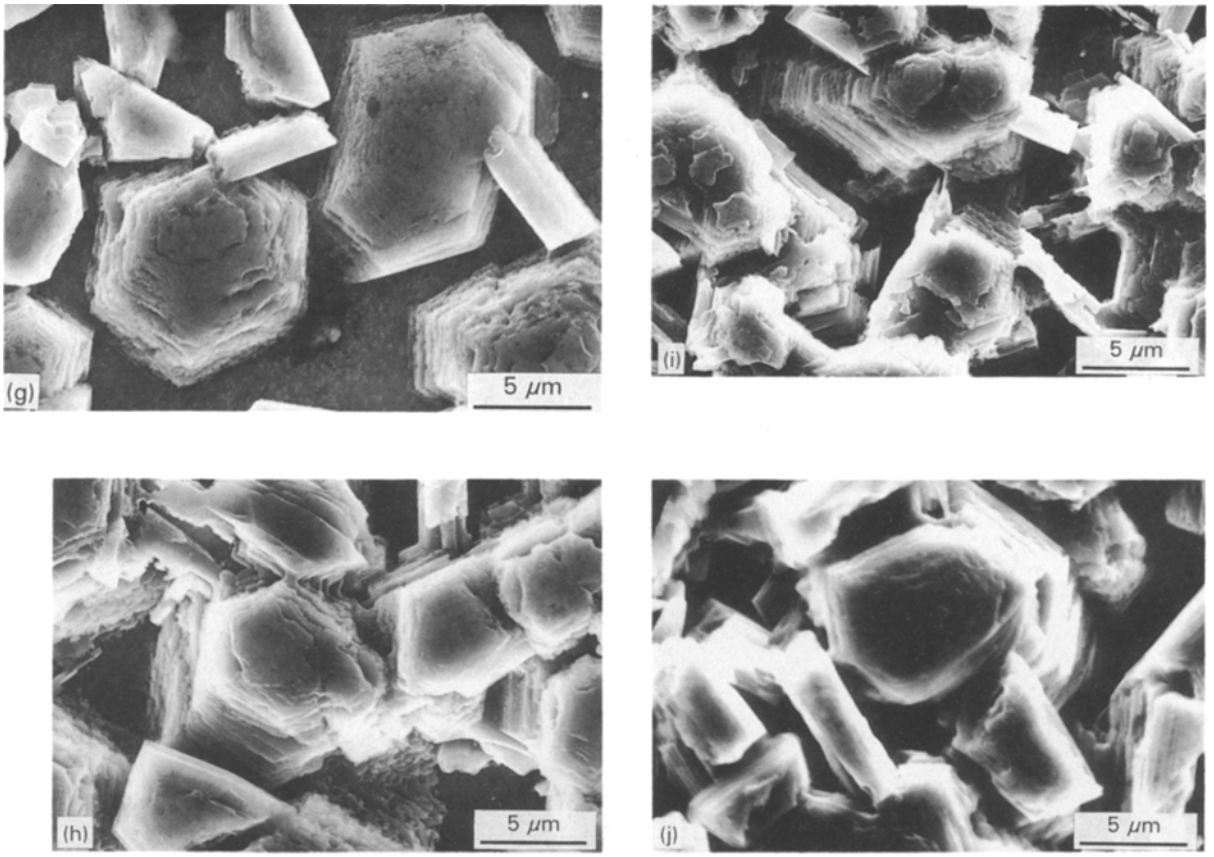

Figure 7 (Continued)

however, supersaturation conditions for the nucleation of aluminium carbide are realized and Al_4C_3 crystallites appear at the Al/SiC interface (Fig. 8b). This results in the creation of a carbon-concentration gradient, in liquid aluminium, between places directly in contact with SiC (where the carbon content approaches that of point B) and growing faces of Al_4C_3 crystallites that are in equilibrium with a solution having a carbon content lying on the curve AC (Fig. 8a). It is the existence of such a concentration gradient that renders possible further consumption of SiC and further growth of Al_4C_3 crystals by migration of carbon atoms diffusing in the liquid phase. These places where SiC is directly exposed to liquid aluminium correspond to the flat surface observed by SEM on the Si face after a reaction time of 15 min. As for the islands emerging from this flat surface, they correspond to the basal plane of Al_4C_3 crystallites which have nucleated onto the SiC substrate surface in the early stage of the reaction and which protect this surface against dissolution (Fig. 8c). As the reaction proceeds further, Al_4C_3 cyrstallites extend laterally over each island, protecting a larger area, whereas erosion by dissolution continues in non-protected places (Fig. 8d). Then, when the reaction time increases, the islands take pyramidal shapes whereas the dissolution valleys become deeper.

Such a decomposition reaction can proceed as long as the silicon content in the liquid phase remains lower than 4.7 at %, a value corresponding to the composition at 1000 K at point C (Fig. 8a). This is far from the case in our experimental conditions, and only kinetic factors could impede further decomposition of the SiC substrates. Accordingly, for a reaction time of 15 h (Fig. 7c and h), the roughness of the substrate surface increased, it was of order 4 μm. The dissolution valleys also became deeper, with only some of them retaining a flat bottom. It can be noted that Al_4C_3 crystals grown at the Al/SiC interface were not bigger but they were in greater number than previously, which indicates that new seeds nucleated on those formed previously and that they tend to join together, forming a non-continuous layer about 3 μm thick.

For a reaction time of 150 h, the Si face of the SiC substrate is entirely coated by a dense and continuous Al_4C_3 layer with a thickness of about 3 μm. Except for some rare places where dissolution dug narrow and deep valleys, the SiC substrate surface was no longer in contact with liquid aluminium. At this point, its average roughness was of order 5 μm. Then, decomposition of the Si face of α-SiC single crystals by a dissolution–precipitation mechanism was no longer possible. Further growth of Al_4C_3 could only progress by solid-state diffusion of Si, Al or C through the reaction layer. The results obtained for a reaction time of 1500 h at 1000 K show that the thickness of the Al_4C_3 reaction layer (3–4 μm) and the roughness of the Si surface (about 6 μm) only slightly increased, compared with those values measured for a reaction time of 150 h, whereas the silicon content in the liquid phase was still lower than 1 at %. It can thus be concluded that the rate at which the Si surface of α-SiC single crystals can be decomposed via such a solid-state diffusion mechanism is almost zero at

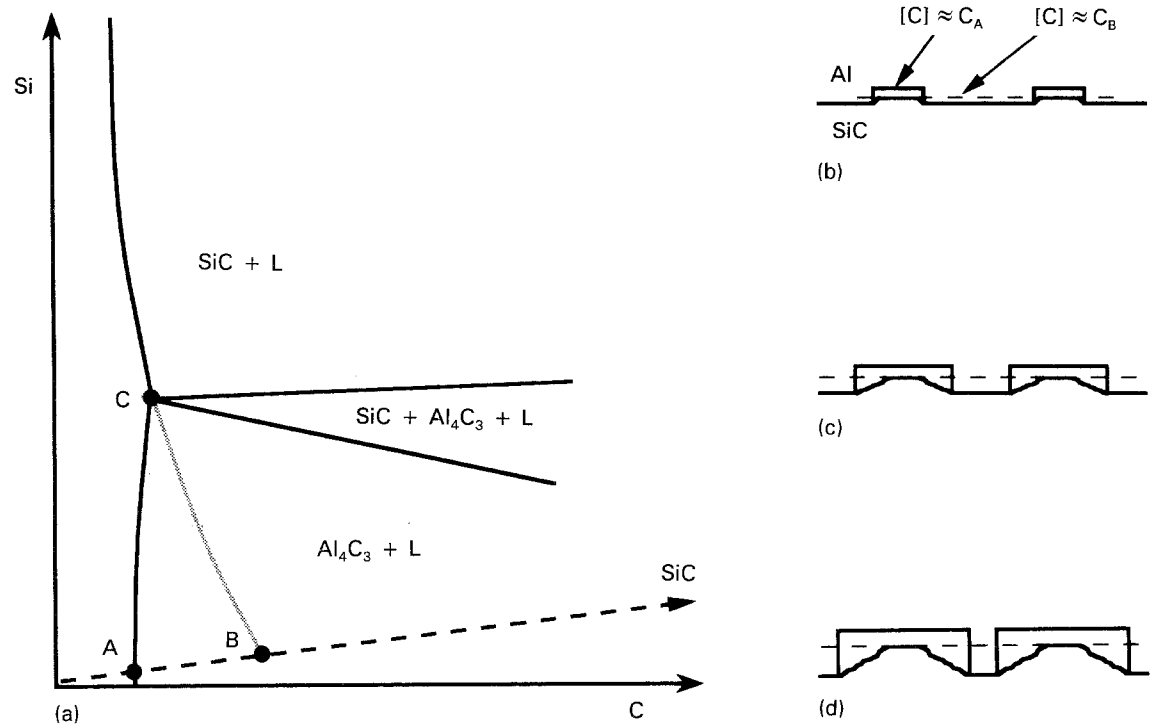

Figure 8. Schematic description of the dissolution– precipitation mechanism occurring at the Si face of α-hexagonal SiC crystals exposed to liquid aluminium in excess: (a) the aluminium-rich partial Al–C–Si section at 1000 K; (b), (c) and (d) nucleation and growth of Al_4C_3 crystals.

1000 K. This explains why the Si surface is very efficiently protected in places where Al_4C_3 crystallites have nucleated in the early stage of the reaction process and justifies the surface roughness chosen in Fig. 9 to represent the variation with the reaction time of the average depth on which SiC was decomposed at 1000 K.

The sharp edges and the geometrical outlines of the islands as well as the flat bottom of the dissolution valleys observed at different reaction times (Fig. 7f to j) reveal the main crystalline orientations of the SiC substrate. This indicates that dissolution proceeds in a very uniform manner for a given orientation but that the dissolution rate may change with the crystallographic orientation of the α-SiC substrate. Orientation relationships also exist between the growing Al_4C_3 crystals and the SiC substrate. A study of the Al/SiC interface by TEM has shown that the [0 0 0 1] axis of several Al_4C_3 crystals was parallel to the [0 0 0 1] axis of the 6H or 15R polytyps of the underlying α-SiC substrate [23]. This will be illustrated in the following section.

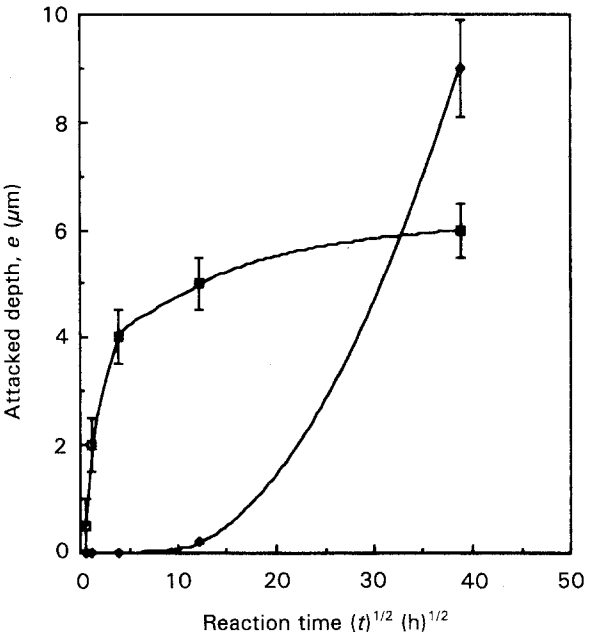

Figure 9. Chemical interaction at 1000 K between Al and SiC showing the variation with the reaction time, t (parabolic coordinates), of the average depth, e, on which the Si and C faces of α-hexagonal SiC single crystals are decomposed: (■) Si face, and (◆) C face.

3.2.2. Polished C surfaces reacted at 1000 K

Fig. 10a to g shows the typical interface and surface morphologies of C polished surfaces reacted under the same experimental conditions as previously, i.e. heated at 1000 K for 15 min to 1500 h.

For reaction times shorter or equal to 150 h, the Al/SiC interface remains straight and the presence of any Al_4C_3 crystallite cannot be detected. After aluminium etching, the surface of the C face appears quite flat when observed by SEM and only a grazing illumination of this surface can reveal nascent dissolution figures with hexagonal shapes at a reaction time of 150 h, when examined by optical metallography. These observations are consistent with the AES results previously obtained and confirm that decomposition of α-SiC single crystals starts much more slowly at the C face then at the Si face.

For a very long reaction time (1500 h), however, large dissolution steps (with a height that can attain 10 μm, i.e. higher than at the Si face under the same conditions) are visible at the C face in transverse

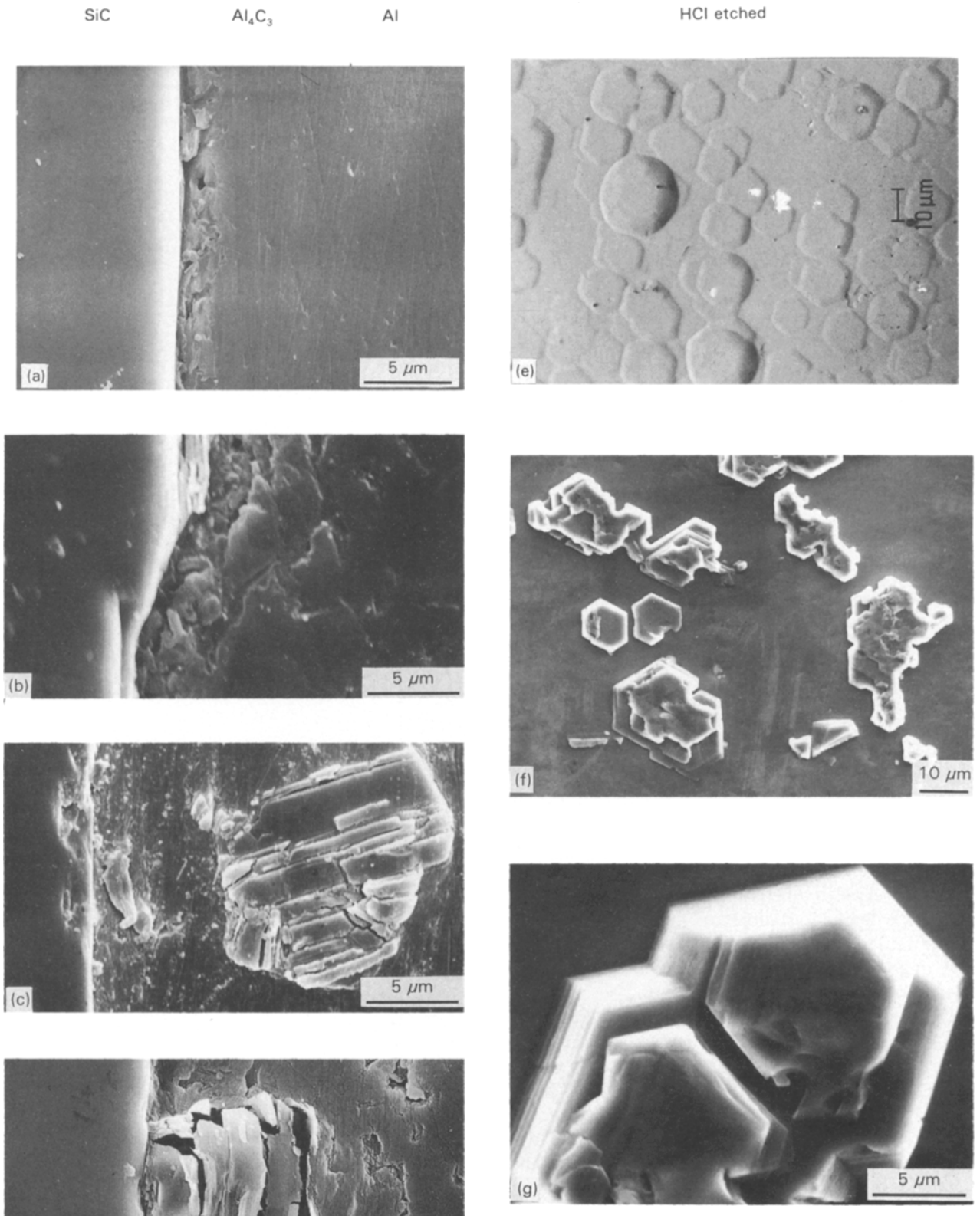

Figure 10. Reaction at 1000 K between the C face of α-hexagonal SiC crystals and liquid aluminium. (a)–(d) transverse section of the Al/SiC interface ; and (e)–(g) morphology of the C face after chemical dissolution of Al and Al_4C_3 (a), (e) 150 h; and (b), (c), (d), (f), and (g) 1500 h.

section (Fig. 10b). Surprisingly, a true Al/SiC interface is generally observed, and if many Al_4C_3 crystals can be found near the metal/carbide interface (Fig. 10c) only few of these crystals are in direct contact with the SiC substrate. One of these crystals can be seen in Fig. 10d: it can be noted that such crystals exhibit a globular shape and tend to grow vertically in the liquid phase rather than spreading horizontally on the substrate surface. After acidic etching, large SiC pyramids emerging on a fairly flat bottom are visible on the C surface (Fig. 10f and g). The pyramids correspond to the rare places where Al_4C_3 crystals have grown and

protected the underlying substrate, whereas the fairly flat bottom corresponds to the main parts of the C surface that have been decomposed by dissolution in liquid aluminium.

From these observations, it is obvious that dissolution of the SiC substrate proceeds at a much slower rate at the C face than at the opposite Si surface. But while the Si surface is rapidly covered by a layer of Al_4C_3 crystals which protect it against further attack, the major part of the C surface remains in direct contact with liquid aluminium and continues to dissolve at a low but constant rate. This is the reason why, for very long reaction times, the quantity of SiC decomposed is larger at the C face than at the Si face, as shown by Fig. 9.

3.2.3. *Unpolished Si and C faces reacted at 1000 K*

Another series of Al–SiC samples (parallelepipedic rods) was prepared from SiC crystals, the Si and C faces of which were not mechanically polished as previously but were just etched in a dilute hydrofluoric-acid solution and dried prior to cold pressing with aluminium. After heat treatment at 1000 K for 1.5, 15 and 150 h, these samples were cut perpendicularly to the Si and C faces and examined by SEM. Typical photographs of such transverse sections are presented in Fig. 11.

It can be seen that the chemical behaviour in liquid aluminium of unpolished Si and C faces is almost the same as that of mechanically polished surfaces: after

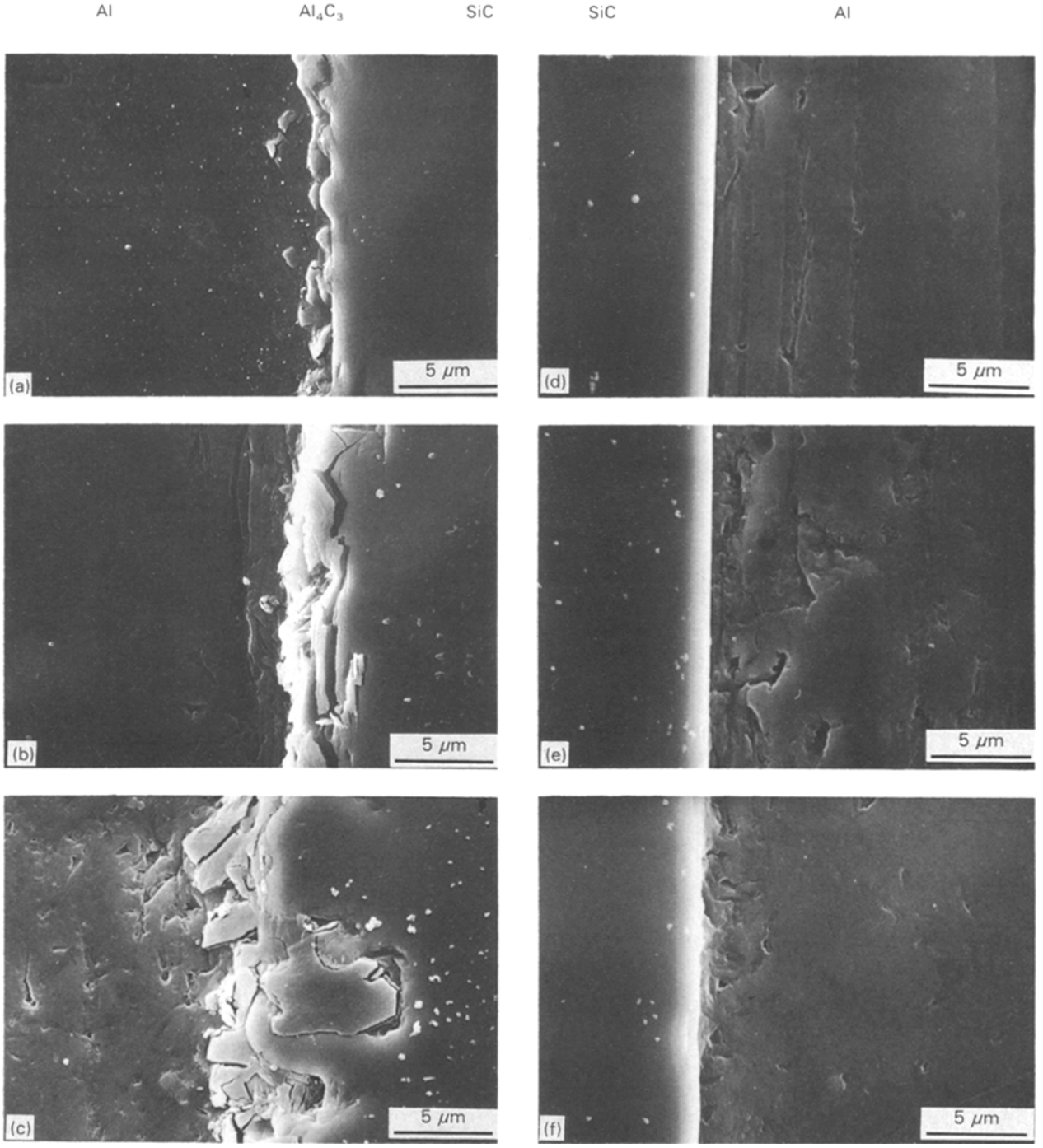

Figure 11. Transverse sections of the metal/carbide interface after heating at 1000 K for 1.5, 15 and 150 h α-hexagonal SiC crystals in aluminium. (a)–(c) unpolished Si face; (d)–(f) unpolished C face: (a), (d) 1.5 h; (b), (e) 15 h; and (c), (f) 150 h.

150 h at 1000 K, the Si face is entirely covered with a continuous layer of Al_4C_3 crystals grown via a dissolution–precipitation mechanism, whereas the C face appears unattacked. It can, however, be noted that reaction at the Si face starts more rapidly for a polished surface than for an unpolished one. This may be due to the fact that mechanical abrasion enhances the chemical reactivity of this face by surface amorphization.

3.2.4. Effect of temperature

The influence of temperature on the mechanism and kinetics of decomposition of α-SiC crystals by aluminium was studied by reacting mechanically polished Si and C faces for 150 h at 930 and 1100 K. Transverse sections of the metal/carbide interface and chemically etched substrate surfaces are presented in Fig. 12 for the Si face and in Fig. 13 for the C face.

Results obtained for the Si face at 930 K (Fig. 12) show that a reaction has occurred, although pure aluminium is still in the solid state (the melting point of Al is 933 K). On account of the typical morphologies exhibited by the reaction zone and the substrate surface, it is clear that this reaction has proceeded according to the same dissolution– precipitation mechanism as that previously observed at 1000 K. This indicates that a liquid phase has transiently formed in the vicinity of the metal/carbide interface by dissolution of silicon in the metal matrix. Al_4C_3 crystals grown at 930 K on the Si face form a continuous layer, but when compared with results obtained at 1000 K after the same reaction time this layer is thinner (2 μm instead of 3 μm) and the SiC roughness is smaller (3 μm instead of 5 μm). After 150 h at 1100 K, the Si face of the SiC substrate is much more severely attacked than at 1000 K. A first layer of Al_4C_3 platelets has grown onto the substrate surface in the early stage of the interaction. The protection from this first layer was, however, not sufficient and liquid aluminium continued to dissolve SiC at a reduced rate. A second Al_4C_3 layer then covered and passivated the SiC substrate. At this stage, the apparent roughness of the SiC surface is of order 8 μm instead of 5 μm at 1000 K (Fig. 12).

The C face (Fig. 13) appears unattacked after 150 h at 930 K whereas results obtained at 1100 K are almost identical to those obtained from 1500 h at 1000 K, i.e. formation of large dissolution steps and preferential growth of Al_4C_3 crystals in the liquid phase without passivation.

The mechanism of the chemical decomposition of α-SiC single crystals by aluminium in excess, as well as the differences in behaviour previously observed at

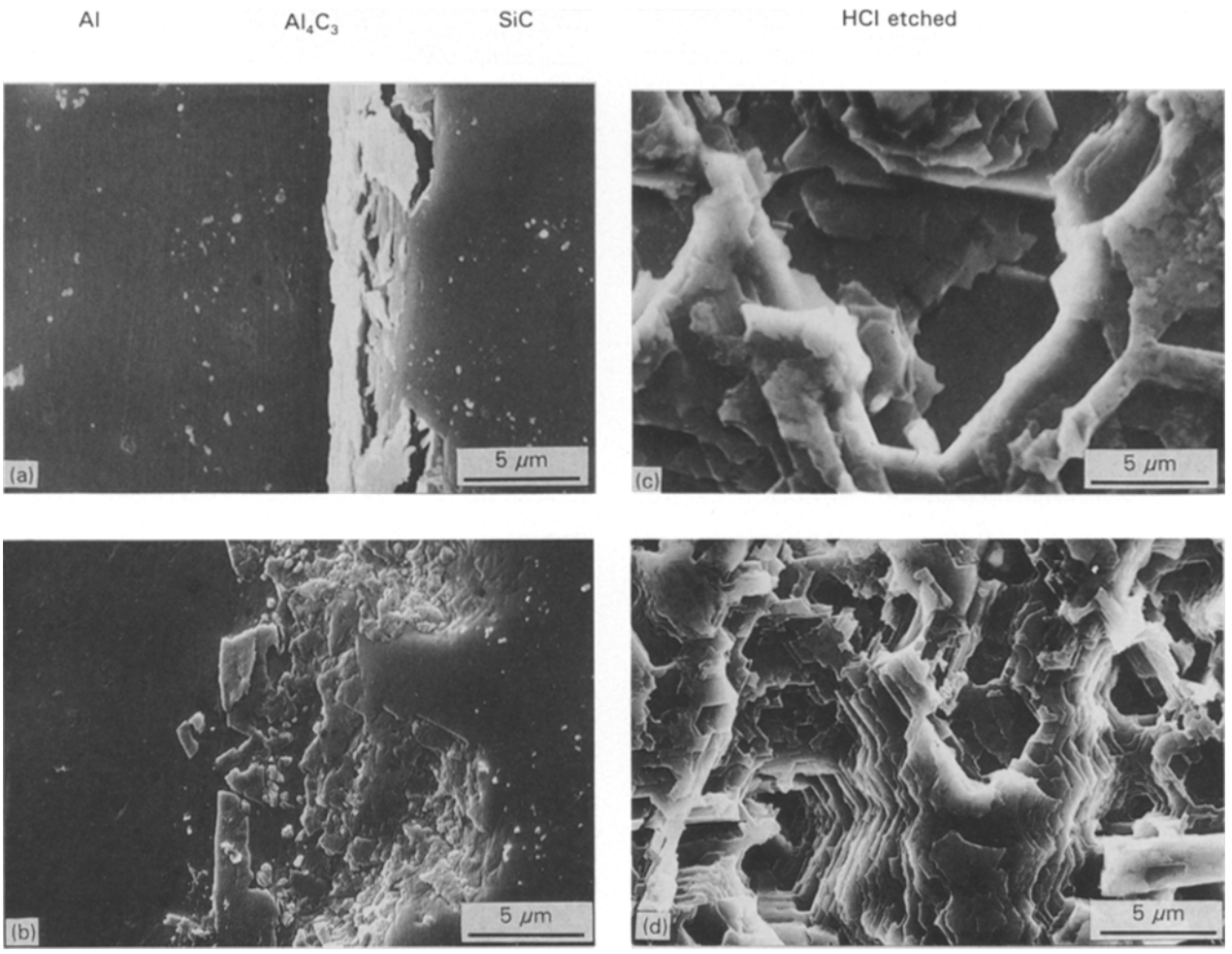

Figure 12 Si face of α-hexagonal SiC crystals reacted with aluminium for 150 h. (a), (b): Metal/carbide interface. (c), (d): Si surface morphology after chemical dissolution of Al and Al_4C_3. (a), (c) 930 K; and (b), (d) 1100 K.

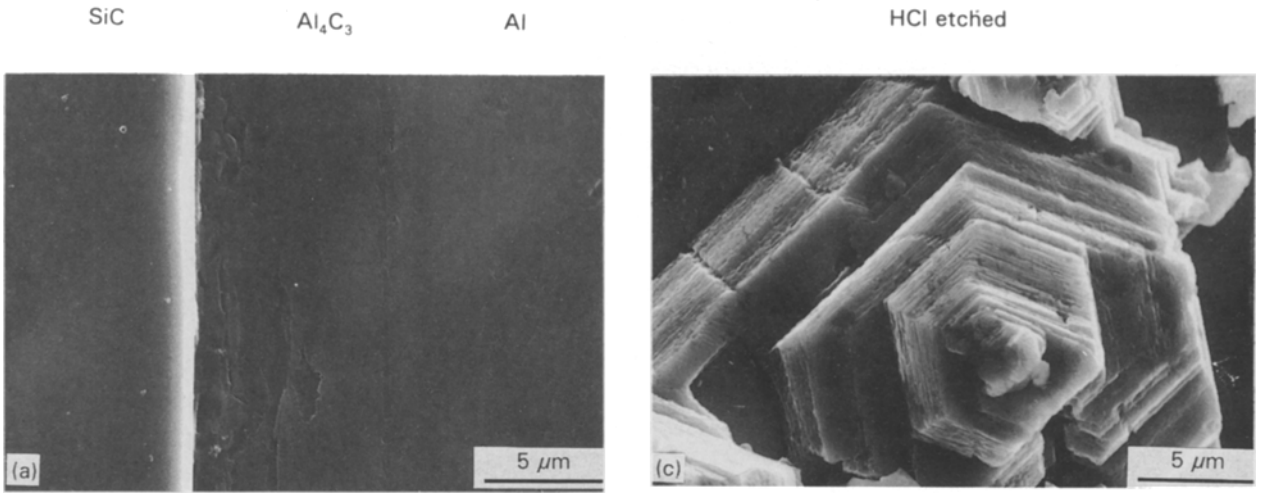

Figure 13. C face of α-hexagonal SiC crystals reacted with aluminium for 150 h at 930 and 1100 K. Metal/carbide interface (a) 930 K, (b) 1100 K. and (c) the C surface morphology after chemical dissolution of Al and Al_4C_3.

1000 K for the Si and C faces, are not fundamentally affected by temperature modifications. As shown by Fig. 14, increasing the reaction temperature simply results in a faster decomposition rate at the C face and in a delayed passivation at the Si face, which would suggest that the rate of dissolution at this face increases faster than the rate at which Al_4C_3 crystals can coat it by lateral extension.

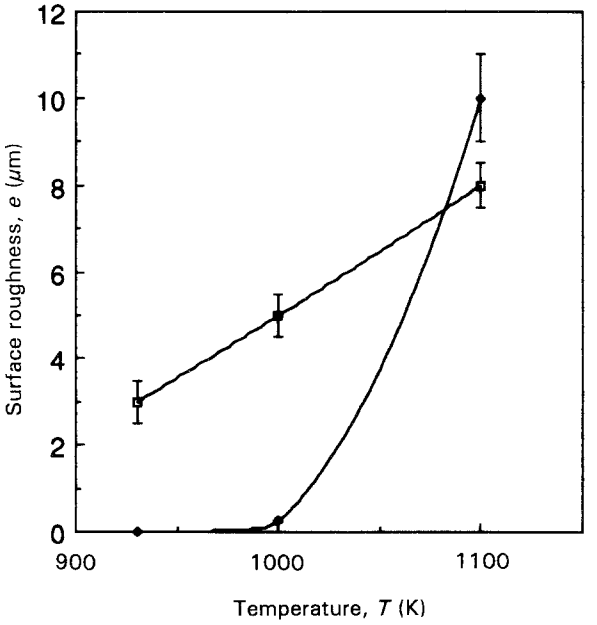

Figure 14. Temperature dependence of the roughness, e, of the Si and C surfaces of α-hexagonal SiC crystals reacted for 150 h with aluminium: (□) Si face, and (◆) C face.

3.2.5. Randomly oriented faces or fractures

SEM observations of the Al/SiC interface were made on samples heat treated for 150 h at 1000 K, in places where the surface of the α-SiC substrate was not perpendicular to its c-axis. It can be seen in Fig. 15 that the chemical behaviour of randomly oriented faces of α-SiC crystals is not very different from that of the Si face. The former faces appear to dissolve in liquid aluminium at least as fast as the latter and in both cases, Al_4C_3 crystals have grown from the liquid phase onto the surface substrate. The fact that most of these Al_4C_3 crystals appear in the form of platelets that have preferentially extended in directions perpendicular to the c-axis of the underlying SiC substrate illustrates the α-SiC/Al_4C_3 orientation relationships previously found by TEM. Due to the existence of these orientation relationships, and of preferential growth directions, formation of a continuous and protective Al_4C_3 layer will be easier on the Si face than on randomly oriented faces, which is effectively observed in Fig. 15. Following this reasoning, passivation on the C face should also be favoured, but

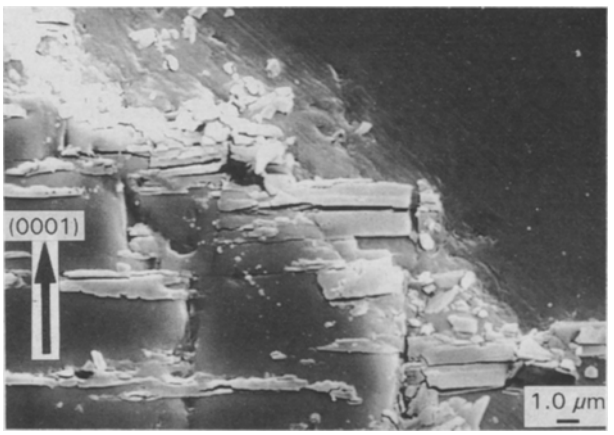

Figure 15. Al_4C_3 platelets grown on randomly oriented faces of the terminal part of α-hexagonal SiC crystals exposed to aluminium attack for 150 h at 1000 K.

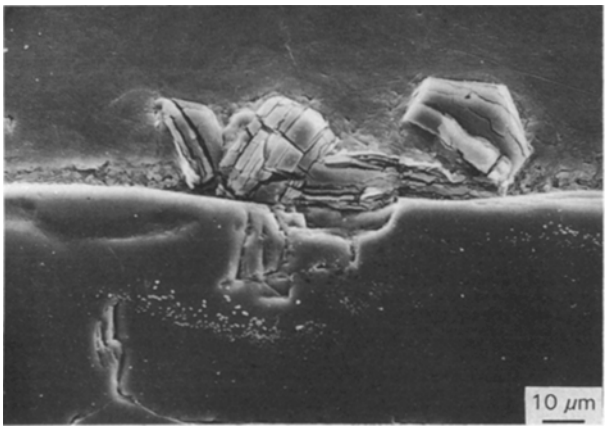

Figure 16. Al_4C_3 crystals exceptionally grown on a surface defect at the C face of an α-hexagonal SiC substrate reacted with aluminium for 150 h at 1000 K.

exactly the contrary is observed. This leads to the consideration that the particular behaviour of this face mainly originates from the fact that fixation of Al_4C_3 seeds on it is impossible, except in places where important surface defects reveal randomly oriented faces. Such a place in which Al_4C_3 crystals have fixed and developed is shown in Fig. 16.

4. Conclusion

Results obtained in the present work show that the chemical interaction at temperatures ranging from 930 to 1100 K between solid or liquid aluminium and α-hexagonal silicon carbide crystals always proceeds via a dissolution–precipitation mechanism. This mechanism involves the migration of carbon atoms by liquid-phase diffusion from places where the SiC surface is in direct contact with the metal matrix to the growing faces of Al_4C_3 crystals located at or near the metal/carbide interface. The silicon liberated in this reaction dissolves in aluminium in excess, forming a liquid Al–Si alloy.

The rate at which such a decomposition reaction proceeds, as well as the morphology of the resulting reaction zone, greatly depends, however, on the polarity of the substrate surface exposed to aluminium attack. The (0 0 0 1) Si face and the randomly oriented faces behave in a similar manner. These faces dissolve at a rather fast rate in aluminium and, correlatively, Al_4C_3 crystallites nucleate onto the SiC surface with their *c*-axis preferentially oriented in a direction parallel to the *c*-axis of the substrate. Lateral extension of these crystallites results in the formation of an adherent and continuous layer of Al_4C_3 crystals that very efficiently protect the underlying substrate from further decomposition. Due to these preferential germination and growth orientations, passivation takes place sooner at the Si face than at randomly oriented faces. As for the $(0\,0\,0\,\bar{1})$ C face, it exhibits a very particular behaviour: it dissolves at a much slower rate than any other face (six to ten times slower); but, as Al_4C_3 crystals cannot nucleate or remain fixed onto this face, passivation never occurs. Consequently, if exposed for a very long time to aluminium attack, the C face will appear more damaged than any other face.

Large differences in the chemical behaviour of the Si and C faces of α-hexagonal SiC single crystals have also been reported in the case of oxidation in dry oxygen [19–20], etching by molten Na_2CO_3 [18] and epitaxial growth from a gaseous mixture [25]. Oxidation, etching and epitaxy were found, however, to proceed faster at the C surface than at the Si surface, leading some authors to conclude that the former was chemically more reactive than the latter. In the case of aluminium attack, it is the Si face that must be considered as the more reactive, although the C face may be severely damaged under special conditions (long-time or high-temperature reactions). It can thus be assumed that if, as a general rule, the polar structure of α-hexagonal SiC single crystals strongly influences their chemical behaviour, the reactivity of each face as well as the reaction mechanism and kinetics also depends highly on the chemical reagent.

References

1. V. BERMUDEZ, *Appl. Phys. Lett.* **42** (1983) 70.
2. T. ISEKI, T. MARUYAMA and T. KAMEDA, *J. Mater. Sci.* **34** (1984) 241.
3. E. NAKATA, K. SATO and Y. KAGAWA, *J. Mater. Sci. Lett.* **3** (1984) 611.
4. R. J. ARSENAULT and C. S. PANDE, *Scripta Metall.* **18** (1984) 1131.
5. J. C. VIALA, P. FORTIER, C. BERNARD and J. BOUIX, *C. R. Acad. Sci. Paris, Ser.* 2 **299** (1984) 777.
6. S. R. NUTT and F. E. WAWNER, *J. Mater. Sci.* **20** (1985) 1953.
7. T. G. NIEH, J. WADSWORTH and D. J. CHELLMANN, *Scripta Metall.* **19** (1985) 181.
8. L. PORTE, *J. Appl. Phys.* **60** (1986) 635.
9. J. C. VIALA, P. FORTIER, B. BONNETOT and J. BOUIX, *Mater. Res. Bull.* **21** (1986) 387.
10. T. A. CHERNYSHOVA and A. V. REBROV, *J. Less-Common Metals* **117** (1986) 203.
11. K. KANNIKESWARAN and R. Y. LIN, *J. Metals* **39** (1987) 17.
12. V. M. BERMUDEZ, *J. Appl. Phys.* **63** (1988) 4951.
13. D. J. LEE, M. D. VAUDIN, C. A. HANDWERKER and KATTNER, *Mater. Res. Soc. Symp. Proc.* **120** (1988) 357.
14. D. J. LLOYD, H. LAGACE, A. MCLEOD and P. L. MORRIS, *Mater. Sci. Engng. A* **107** (1989) 73.
15. L. L. ODEN and R. A. MCCUNE, *Metal. Trans. A* **18** (1987) 2005.
16. H. L. LUKAS in "Ternary alloys", edited by G. PETZOW and G. EFFENBERG (VCH Verlags, Weinheim, FRG, 1988) p. 540.
17. J. C. VIALA, P. FORTIER and J. BOUIX, *J. Mater. Sci.* **25** (1990) 1842.
18. R. MUEHLHOFF, W. J. CHOYKE, M. J. BOSACK and J. T. YATES, *J. Appl. Phys.* **60** (1986) 2842.
19. R. C. A. HARRIS, *J. Amer. Ceram. Soc.* **58** (1975) 7.
20. J. A. COSTELLO and R. E. TRESSLER, *J. Amer. Ceram. Soc.* **69** (1986) 674.
21. V. LAURENT, D. CHATAIN and N. EUSTATHOPOULOS, *J. Mater. Sci.* **22** (1987) 244.
22. V. LAURENT, Thesis, INPG, Grenoble, France, 4 November (1988).
23. S. D. PETEVES, P. TAMBUYSER, P. HELBACH, M. AUDIER, V. LAURENT and D. CHATAIN, *J. Mater. Sci.* **25** (1990) 3765.
24. C. J. SIMENSEN, *Metall. Trans. A* **20** (1989) 191.
25. S. NISHINO, H. MATSUNAMI and T. TANAKA, *J. Crystal Growth* **45** (1978) 144.

Received 27 April 1992
and accepted 24 February 1993